Inorg. Chem. **2007**, *46*, 2459–2470

Water Exchange on Seven-Coordinate Mn(II) Complexes with Macrocyclic Pentadentate Ligands: Insight in the Mechanism of Mn(II) SOD Mimetics

Anne Dees, Achim Zahl, Ralph Puchta, Nico J. R. van Eikema Hommes, Frank W. Heinemann, and Ivana Ivanović-Burmazović*

Institute for Inorganic Chemistry, University of Erlangen-Nürnberg, Egerlandstrasse 1, 91058 Erlangen, Germany

Received September 27, 2006

Seven-coordinate manganese(II) complexes $[Mn(L)(H_2O)_2]^{2+}$, where L represents an equatorial pentadentate macrocyclic ligand with five nitrogen donor atoms, were studied with regard to their acid–base properties, water-exchange rate constants, and corresponding activation parameters ($\Delta H^{\ddagger}$, $\Delta S^{\ddagger}$, and $\Delta V^{\ddagger}$). Three of the studied complexes without imine bonds in the macrocyclic ligand are proven superoxide dismutase (SOD) mimetics. Their water-exchange parameters were compared with those of the imino groups containing complex $[Mn(L1)(Cl)_2]$ (dichloro-2,13-dimethyl-3,6,9,12,18-pentaazabicyclo[12.3.1]-octadeca-1(18),2,12,14,16-pentaenemanganese(II)), which does not show SOD activity. In addition the X-ray crystal structure of a new complex, dichloro-2,6-bis[*1*-(2-(*N*-methylamino)-ethylimino)ethyl]pyridine-manganese(II) $[Mn(L2)(Cl)_2]$, which is the acyclic analog of $[Mn(L1)(Cl)_2]$, is reported. Stability constants of the complexes and the pK_a values of the ligands were measured by potentiometric titration. The titrations of $[Mn(L1)(H_2O)_2]^{2+}$ and $[Mn(L2)(H_2O)_2]^{2+}$ led to complicated species distribution curves because of their ligands containing imine bonds. Water exchange was measured by temperature- and pressure-dependent ^{17}O NMR techniques. In addition to the measurements on $[Mn(EDTA)(H_2O)]^{2-}$ and its derivatives, this is the only study of water exchange on seven-coordinate manganese complexes. The water exchange rate constants vary between 1.6×10^7 s^{-1} and 5.8×10^7 s^{-1} at 25 °C and are mainly controlled by the π-acceptor abilities of the ligands. The exchange rate constant of the diaqua-1,4,7,10,13-pentaazacyclopentadecanemanganese(II) $[Mn([15]aneN_5)(H_2O)_2]^{2+}$ complex seems to be even higher but could not be exactly determined. On the basis of the obtained activation parameters, the exchange mechanism of the studied seven-coordinate manganese(II) complexes follows a dissociative pathway (I_d mechanism). DFT calculations (UB3LYP/LANL2DZp) were performed to obtain the energy required for the dissociation of the coordinated water molecule, that is, the energy difference between the starting seven-coordinate complex and a six-coordinate intermediate. The results have been discussed in terms of the catalytic mechanism of the proven SOD mimetics.

Introduction

The superoxide radical anion $O_2^{\bullet -}$ is formed as a byproduct of normal cellular respiration. Its decomposition produces further undesired harmful species like the hydroxyl radical and hydrogen peroxide. To keep the formation of these species under control, nature has created a family of enzymes which remove them from the cellular environment. One of these, superoxide dismutase (SOD), catalyzes the disproportionation of superoxide to dioxygen and hydrogen peroxide, which then is decomposed via catalase to water and dioxygen.[1] There are three classes of SOD enzymes found in nature: a Cu/Zn-containing protein in eukaryotic and some prokaryotic cells, iron and manganese SODs in prokaryotic organisms and mitochondria, respectively, and nickel-containing SODs in some prokaryotes.[1,2] However, since the natural enzymes show some drawbacks as therapeutic agents,[3] different low molecular weight catalysts

* To whom correspondence should be addressed. E-mail: ivana.ivanovic@chemie.uni-erlangen.de. Phone: +49 9131 8527391. Fax: +49 9131 8527387.

(1) Cass, A. E. G. Superoxide Dismutases. In *Metalloproteins, Part I: Metal Proteins with Redox Roles*; Harrison, P., Ed; Verlag Chemie: Weinheim, Germany, 1985; pp 121−156.

10.1021/ic061852o CCC: $37.00
Published on Web 02/28/2007

Scheme 1. Catalytic Cycle for the Seven-Coordinate SOD Mimetics as Proposed in Literature.[10,12,14,20] [a]

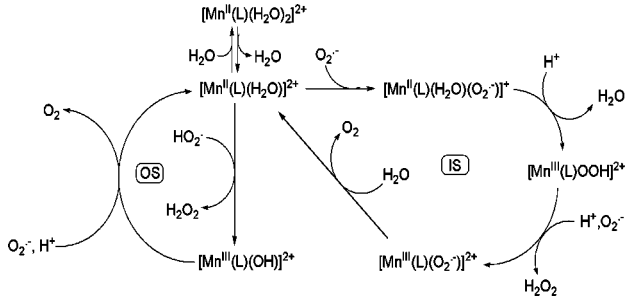

[a] OS = outer-sphere pathway; IS = inner-sphere pathway.

(synzymes) have been synthesized in attempt to mimic their structure and functionality.[3−10] The most active SOD mimetics known to date are seven-coordinate Mn(II) complexes with macrocyclic ligands derived from C-substituted pentaazacyclopentadecane [15]aneN$_5$.[3,11,12] These complexes have potential utility for the treatment of diseases characterized by the overproduction of superoxide, for example, ischemia reperfusion injury, inflammatory deseases, and vascular deseases.[10,13−15] Those with high catalytic activity and chemical stability were chosen for pharmaceutical studies and are the first SOD mimetics which entered clinical trials.[3,11,16−19] A catalytic cycle for the seven-coordinate Mn(II) complexes which consists of two reaction pathways, a pH-independent inner-sphere pathway and a pH-dependent outer-sphere one, was reported and is summarized in Scheme 1.[10,12,14,20] It was claimed that for the pH-independent

Scheme 2. Ligands and Complexes

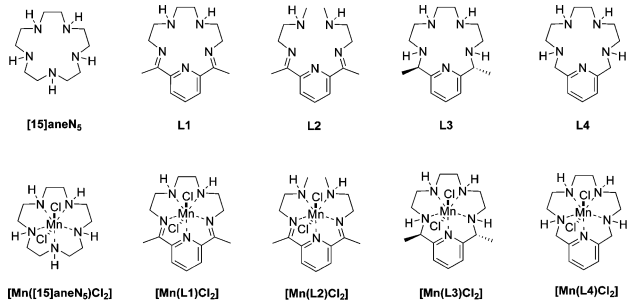

pathway, which contains inner-sphere binding of superoxide to a vacant coordination site on the manganese center, the rate of formation of a vacant axial coordination site is the rate-determining step, whereas for the pH-dependent process the proton-coupled electron-transfer step was found to be rate limiting.[10,14,15] Another catalytic cycle for the reaction of five-coordinate manganese complexes with superoxide in which the oxidation of superoxide follows an outer-sphere pathway and the reduction of superoxide to hydrogen peroxide follows an inner-sphere pathway, involving a manganese(II)−superoxide adduct as a transient, was proposed by a group in France recently.[9]

The loss of one water ligand from the seven-coordinate complexes is the first step in this reaction cascade (Scheme 1) to form the corresponding six-coordinate intermediate which can enter the catalytic cycle. It was assumed that the release of water and the formation of a six-coordinate intermediate is the rate-limiting step, and the catalytic rate constants for the inner-sphere pathway were compared with the water exchange rate constant for the $[Mn(H_2O)_6]^{2+}$ ion.[10,12,14] Water exchange on $[Mn(H_2O)_6]^{2+}$ follows an interchange associative (I_a) mechanism based on $\Delta V^{\ddagger}$ with a seven-coordinate intermediate and was measured to be $2.1 \times 10^7\ s^{-1}$.[21] The exchange of the aqua ligands of the seven-coordinate complexes (eq 1) however should follow a dissociative pathway with a six-coordinate intermediate, and it is thus far unknown how the exchange rate constant of these complexes is influenced by the structure of the ligands.

$$[MnL(H_2O)_2] + H_2O^* \rightleftharpoons [MnL(H_2O)(H_2O)^*] + H_2O \quad (1)$$

We report here a detailed study of the acid−base properties of some pentaaza macrocyclic seven-coordinate manganese(II) complexes (Scheme 2) in aqueous solution and their water-exchange rate constants and activation parameters measured by temperature- and pressure-dependent ^{17}O NMR techniques, which were performed to gain more insight into the mechanism and to better understand the details of the influence of the ligand structure on the lability, that is, reactivity of the complexes. Three of them, without the imine groups in the macrocyclic ligand, are proven SOD mimetics.[13,18] It was reported that the $[Mn(L1)Cl_2]$ complex was SOD inactive, probably because of its low conformational

(2) Barondeau, D. P.; Kassmann, C. J.; Bruns, C. K.; Tainer, J. A.; Getzoff, E. D. *Biochemistry* **2004**, *43*, 8038−8047.
(3) Muscoli, C.; Cuzzocrea, S.; Riley, D. P.; Zweier, J. L.; Thiemermann, C.; Wang, Z.-Q.; Salvemini, D. *Brit. J. Pharmacol.* **2003**, *140*, 445−460.
(4) (a) Ohtsu, H.; Shimazaki, Y.; Odani, A.; Yamauchi, O.; Mori, W.; Itoh, S.; Fukuzumi, S. *J. Am. Chem. Soc.* **2000**, *122*, 5733−5741. (b) Li, D.; Li, S.; Yang, D.; Yu, J.; Huang, J.; Li, Y.; Tang, W. *Inorg. Chem.* **2003**, *42*, 6071−6080. (c) Durackova, Z.; Labuda, J. *J. Inorg. Biochem.* **1995**, *58*, 297−303. (d) Liao, Z.; Xiang, D.; Li, D.; Mei, F.; Yun, F. *Synth. React. Inorg. Met.−Org. Chem.* **1998**, *28*, 1327−1341.
(5) Batinic-Haberle, I.; Spasojevic, I.; Hambright, P.; Benov, L.; Crumbliss, A. L.; Fridovich, I. *Inorg. Chem.* **1999**, *38*, 4011−4022.
(6) Zhang, D.; Busch, D. H.; Lennon, P. L.; Weiss, R. H.; Neumann, W. L.; Riley, D. P. *Inorg. Chem.* **1998**, *37*, 956−963.
(7) Yamaguchi, S.; Kumagai, A.; Funahashi, Y.; Jitsukawa, K.; Masuda, H. *Inorg. Chem.* **2003**, *42*, 7698−7700.
(8) Shearer, J.; Long, L. M. *Inorg. Chem.* **2006**, *45*, 2358−2360.
(9) Durot, S.; Lambert, F.; Renault, J.-P.; Policar, C. *Eur. J. Inorg. Chem.* **2005**, 2789−2793.
(10) Riley, D. P.; Weiss, R. H. *J. Am. Chem. Soc.* **1994**, *116*, 387−388.
(11) Salvemini, D.; Wang, Z.-Q.; Zweier, J. L.; Samouilov, A.; Macarthur, H.; Misko, T. P.; Currie, M. G.; Cuzzocrea, S.; Sikorski, J. A.; Riley, D. P. *Science* **1999**, *286*, 304−306.
(12) Riley, D. P.; Schall, O. F. *Adv. Inorg. Chem.* **2007**, *59*, 233−263.
(13) Riley, D. P.; Henke, S. L.; Lennon, P. J.; Weiss, R. H.; Neumann, W. L.; Rivers, W. J., Jr.; Aston, K. W.; Sample, K. R.; Rahman, H.; Ling, C.-S.; Shieh, J.-J.; Busch, D. H.; Szulbinski, W. *Inorg. Chem.* **1996**, *35*, 5213−5231.
(14) Riley, D. P; Lennon, P. J.; Neumann, W. L.; Weiss, R. H. *J. Am. Chem. Soc.* **1997**, *119*, 6522−6528.
(15) Aston, K.; Rath, N.; Naik, A.; Slomczynska, U.; Schall, O. F.; Riley, D. P. *Inorg. Chem.* **2001**, *40*, 1779−1789.
(16) Cuzzocrea, S.; Riley, D. P.; Caputi, A. P.; Salvemini, D. *Pharmacol. Rev.* **2001**, *53*, 135−159.
(17) Riley, D. P. *Chem. Rev.* **1999**, *99*, 2573−2587.
(18) Salvemini, D. PCT Int. Appl. WO 98/58636, 1998.
(19) Salvemini, D.; Mazzon, E.; Dugo, L.; Riley, D. P; Serraino, I.; Caputi, A. P.; Cuzzocrea, S. *Br. J. Pharmacol.* **2001**, *132*, 815−827.
(20) Riley, D. P.; Henke, S. L.; Lennon, P. J.; Aston, K. *Inorg. Chem.* **1999**, *38*, 1908−1917.
(21) Ducommun, Y.; Newman, K. E.; Merbach, A. E. *Inorg. Chem.* **1980**, *19*, 3696−3703.

flexibility and, consequently, its low ability to form a six-coordinate pseudo-octahedral intermediate.[10] We have included this complex in our studies to compare its water exchange parameters with those of the more flexible and SOD active $[Mn([15]aneN_5)Cl_2]$, $[Mn(L3)Cl_2]$, and $[Mn(L4)Cl_2]$ complexes. Additionally, we have synthesized and structurally characterized a new $[Mn(L2)Cl_2]$ complex, which is the acyclic analog of $[Mn(L1)Cl_2]$ and consequently has a higher conformational flexibility.

In aqueous solution, two axial chloro ligands are substituted by water molecules. For the study of the water exchange processes, it was necessary first to determine the acid−base properties of the complexes by potentiometric titration to define the pH range where the $[Mn(L)(H_2O)_2]^{2+}$ form of the complexes is the predominant one. The potentiometric titrations of $[Mn([15]aneN_5)(H_2O)_2]^{2+}$ and $[Mn(L4)(H_2O)_2]^{2+}$ were already reported by Riley et al.,[13] and we could confirm their results.

For seven-coordinate 3d metal complexes, a dissociative mode of substitution reactions in general (although there are some exceptions)[22,23] and water exchange in particular with a six-coordinate intermediate is to be expected. In the present study, we have calculated the ΔE between the starting seven-coordinate pentagonal-bipyramidal complex and the lowest-energy six-coordinate pseudo-octahedral structure as an intermediate structure formed after release of a coordinated water molecule.

These studies and the one on $[Mn(EDTA)H_2O]$ and its derivatives[24−27] are the only studies of water exchange in seven-coordinate manganese complexes and are essential for understanding the mechanism of the manganese-containing SOD mimetics.

Experimental Section

Materials and Methods. All reagents and solvents were commercially available (Sigma-Aldrich, Acros Organics, Fluka), were of p.a. grade, and were used without further purification. Anhydrous solvents (purchased from Sigma Aldrich or Acros Organics) were used where needed. Deionized Millipore water was used for all types of measurements. Carlo Erba Elemental Analyzers 1106 and 1108 and a Bruker Avance DPX 300 NMR spectrometer were used for chemical analysis and compound characterization. IR spectra were recorded as KBr pellets on a Mattson FT-IR 60 AR.

Synthesis. The ligand $[15]aneN_5$ (1,4,7,10,13-pentaazacyclopentadecane)[28] and the complex $[Mn(L1)Cl_2]\cdot xH_2O$ (dichloro-2,13-dimethyl-3,6,9,12,18-pentaazabicyclo[12.3.1]-octadeca-1(18),2,12,14,16-pentaenemanganese(II))[29] were synthesized according to literature procedures. For the IR spectra measurements, $[Mn(L1)Cl_2]\cdot xH_2O$ was recrystallized out of the aqueous solutions at pH 5.5 and 9.1. IR (KBr, pH 5.5): $\tilde{\nu}$ [cm^{-1}] = 3424, 3342, 3222, 3070, 2919, 2867, 1646, 1587, 1461, 1419, 1367, 1353, 1257, 1197, 1105, 1045, 817, 547. IR (KBr, pH 9.1): $\tilde{\nu}$ [cm^{-1}] = 3424, 3342, 3222, 3070, 2964, 2912, 2869, 1646, 1587, 1456, 1415, 1376, 1351, 1263, 1097, 1025, 800, 482.

Synthesis of Dichloro-1,4,7,10,13-pentaazacyclopentadecane-manganese(II) $[Mn([15]aneN_5)Cl_2]$. This compound was synthesized according to the published procedure.[10] A solution of the $[15]aneN_5$ ligand (0.28 g, 1.3 mmol) and anhydrous manganese(II) chloride (0.16 g, 1.3 mmol) in 20 mL anhydrous MeOH was refluxed under a dry nitrogen atmosphere, and the reaction was followed by thin layer chromatography (SiO_2, CH_2Cl_2/MeOH 80:20, R_f = 0.46, $KMnO_4$). When the plates indicated the absence of $MnCl_2$ (R_f = 0.23), refluxing was stopped, and the solvent was removed in vacuo. The residue was purified by column chromatography (SiO_2, CH_2Cl_2/MeOH 80:20, R_f = 0.46), and the complex was obtained in a 63% yield. Anal. Calcd for $[Mn([15]aneN_5)Cl_2]\cdot H_2O$: C, 33.44; H, 7.58; N, 19.50. Found: C, 34.22, H, 7.46, N, 19.30.

Synthesis of Dichloro-2,6-bis[1-(2-(*N*-methylamino)ethylimino)ethyl]pyridinemanganese(II) $[Mn(L2)Cl_2]$. Methanol solutions of $MnCl_2\cdot 2H_2O$ (2.98 g, 18.4 mmol in 90 mL) and *N*-methylethylenediamine (3.24 mL, 2.72 g, 36.8 mmol in 25 mL) were added to a refluxing methanol solution of 2,6-diacetylpyridine (3.0 g, 18.4 mmol in 210 mL). The deep red solution was refluxed for an additional hour, and then the flask was left standing overnight at room temperature. The solution was evaporated to about 30 mL, and the yellow precipitate was filtered off, washed with small amounts of ethanol, and dried in vacuo. Yield: 4.22 g (53%). Anal. Calcd for $[Mn(L2)Cl_2]\cdot {}^1/_2H_2O\cdot {}^3/_4CH_3OH$: C, 43.56; H, 6.73; N, 16.13. Found: C, 43.89, H, 7.36, N, 16.20.

Synthesis of Dichloro-*trans*-2,13-dimethyl-3,6,9,12,18-pentaazabicyclo[12.3.1]-octadeca-1(18),14,16-trienemanganese(II) $[Mn(L3)Cl_2]$. The $[Mn(L3)Cl_2]$ complex was obtained by reduction of $[Mn(L1)Cl_2]$ with $NaBH_4$ according to the published procedure.[15] One gram (2.0 mmol) of $[Mn(L1)Cl_2]$ was dissolved in 40 mL of anhydrous EtOH under a nitrogen atmosphere, and sodium borohydride (0.6 g, 16 mmol, 8 equiv) was added. The mixture was stirred at 50 °C for 6 h. The solvent was removed, and the excess of $NaBH_4$ was quenched with a solution of 1.27 g LiCl in 60 mL of MeOH. MeOH was removed in vacuo, and water was added to the residue until all solids were dissolved. The aqueous solution was extracted several times with dichloromethane, and the combined organic phases were dried with anhydrous Na_2SO_4. Removal of the solvent gave the desired compound[30] in a 44% yield. Anal. Calcd for $[Mn(L3)Cl_2]\cdot MeOH$: C, 44.25; H, 7.18; N, 16.09. Found: C, 43.97, H, 6.94, N, 15.90.

Synthesis of Dichloro-3,6,9,12,18-pentaazabicyclo[12.3.1]-octadeca-1(18),14,16-trienemanganese(II) $[Mn(L4)Cl_2]$. For the $[Mn(L4)Cl_2]$ complex, the precursor bisimine complex was synthesized first. 2,6-Pyridinedicarboxaldehyde (0.5 g, 3.7 mmol) and manganese chloride (0.6 g, 3.7 mmol) were mixed in about 15 mL of water and warmed up slightly until all solids dissolved; 0.55 mL of triethylenetetramine (0.54 g, 3.7 mmol) was added dropwise. The solution became cloudy and changed color to deep red. The

(22) Ivanovic-Burmazovic, I.; Hamza, M. S. A.; van Eldik, R. *Inorg. Chem.* **2002**, *41*, 5150−5161.
(23) Ivanovic-Burmazovic, I.; Hamza, M. S. A.; van Eldik, R. *Inorg. Chem.* **2006**, *45*, 1575−1584.
(24) Zetter, M. S.; Grant, M. O.; Wood, E. J.; Dodgen, H. W.; Hunt, J. P. *Inorg. Chem.* **1972**, *11*, 2701−2706.
(25) Zetter, M. S.; Dodgen, H. W.; Hunt, J. P. *Biochemistry* **1973**, *12*, 778−782.
(26) Liu, G.; Dodgen, H. W.; Hunt, J. P. *Inorg. Chem.* **1977**, *16*, 2652−2653.
(27) Troughton, J. S.; Greenfield, M. T.; Greenwood, J. M.; Dumas, S.; Wiethoff, A. J.; Wang, J.; Spiller, M.; McMurry, T. J.; Caravan, P. *Inorg. Chem.* **2004**, *43*, 6313−6323.
(28) (a) Kovacs, Z.; Archer, E. A.; Rusell, M. K.; Sherry, A. D. *Synth. Commun.* **1999**, *29*, 2817−2822. (b) Atkins, T. A.; Richman, J. E.; Oettle, W. *F. Org. Synth.* **1978**, *58*, 86−9.
(29) Jiménez-Sandoval, O.; Ramírez-Rosales, D.; Rosales-Hoz, M.; Sosa-Torres, M. E.; Zamorano-Ulloa, R. *J. Chem. Soc., Dalton Trans.* **1998**, 1551−1556.
(30) Liu, G.-F.; Heinemann, F. W.; Ivanović-Burmazović, I. Crystallographic Data in the Cambridge Database. CCDC 258625.

reaction mixture was refluxed for 3 h, cooled down to room temperature, and filtered. Water was removed in vacuo, and the resulting solid was washed with dry diethyl ether, dried in vacuo, and then reduced with sodium borohydride according to the procedure reported above for $[Mn(L3)Cl_2]$. The complex was purified by column chromatography (SiO_2, CH_2Cl_2/MeOH 90:10, $R_f = 0.46$) Yield: 15% calculated from 2,6-pyridinedicarboxaldehyde. Anal. Calcd for $[Mn(L4)Cl_2]\cdot CH_3OH$: C, 41.29; H, 6.68; N, 17.20. Found: C, 40.95, H, 6.34, N, 17.16.

X-ray Crystal Structure Determination for $[Mn(L2)Cl_2]$. Single crystals of $[Mn(L2)Cl_2]$ were obtained by recrystallization of the complex from methanol. A saturated methanol solution of the complex was prepared at room temperature, and the solution was stored in a refrigerator for several days until yellow crystals were obtained. Data collection was performed using a Bruker Nonius Kappa CCD instrument with Mo Kα radiation ($\lambda = 0.71073$ Å) at 100 K. Structure solution and refinement were carried out using the SHELXTL NT 6.12 software package (Bruker AXS, 2002). The structure was solved by direct methods and refined in the space group $P\bar{1}$ using full-matrix least-squares procedures on F^2. The complex crystallizes with 1.78 equiv of methanol and 0.22 equiv of water. All of the solvate molecules are disordered. One of the MeOH molecules shows orientation disorder of the methyl group only (occupancies of C101 and C102 are 50.9(9) and 49.1(9)%) with the OH group O100 being involved in hydrogen bonding to one of the chloro ligands (Cl1). The second MeOH shares its site with a disordered water molecule in a ratio of methanol/water = 78(1):22(1)%. Again, orientation disorder of the methyl group is observed, resulting in occupancies for C201 and C202 of 42(2) and 36(2)%, and the OH group O200 is involved in hydrogen bonding to the other chloro ligand Cl2. The water molecule is split on two sites that are occupied 13(1)% for O2A and 9(1)% for O2B. No hydrogen atoms have been included for the disordered water molecule. With the exception of the two oxygen-bound H atoms of the methanol molecules that were taken from a difference Fourier map and kept fixed during refinement, all other hydrogen atoms are geometrically positioned and allowed to ride on their adjacent atoms; their isotropic displacement parameters have been tied to those of their carrier atoms by a factor of 1.2 or 1.5. A summary of important crystallographic data, data collection, and refinement details for $[Mn(L2)Cl_2]\cdot 0.22\ H_2O\cdot 1.78\ CH_3OH$ is presented in Table 1.

Table 1. Selected Crystallographic Data for $[Mn(L2)Cl_2]\cdot 0.22H_2O\cdot 1.78\ CH_3OH$

empirical formula	$C_{16.78}H_{32.56}Cl_2MnN_5O_2$
fw	462.24
T (K)	100(2)
cryst syst	triclinic
space group	$P\bar{1}$
a (Å)	10.7054(3)
b (Å)	11.0467(6)
c (Å)	11.5675(8)
α (deg)	62.296(5)
β (deg)	78.953(4)
γ (deg)	67.855(3)
V (Å^3)	1121.6(2)
Z	2
ρ_{calcd} (g cm^{-3})	1.369
abs coeff μ (mm^{-1})	0.847
F(000)	486
cryst size (mm)	0.30 × 0.28 × 0.22
θ range	3.53−27.88°
limiting indices	$-14 \le h \le 14$, $-14 \le k \le 14$, $-15 \le l \le 15$
refls collected	32 908
independent reflns	5338 ($R_{int} = 0.0511$)
obsd reflns [$I > 2\sigma(I)$]	4059
completeness to $\theta = 27.88°$	99.8%
abs correction	semiempirical from equiv
T_{min}/T_{max}	0.736/0.835
data/restraints/params	5338/1/293
GOF on F^2	1.027
final wR indices [$I > 2\sigma(I)$]	$R_1 = 0.0353$, $R_2 = 0.0763$
wR indices (all data)	$R_1 = 0.0579$, $R_2 = 0.0830$
largest diff. peak and hole (e Å^{-3})	0.686 and −0.400

Potentiometric Titrations. Potentiometric measurements were performed on a METROHM 702 SM Titrino in a jacketed, airtight glass titration cell equipped with a combined pH glass electrode (METROHM), N_2 inlet and outlet, and a graduated 10 mL microburet (METROHM). Because $NaClO_4$ was used for the adjustment of the ionic strength, the electrode was filled with NaCl instead of KCl to prevent precipitation of $KClO_4$ and was calibrated using three different commercially available standard buffer solutions of pH 4, 7, and 10. A carbonate-free 0.05 M sodium hydroxide or perchloric acid solution were prepared with nitrogen-saturated deionized Millipore water. The NaOH solution was standardized by titrations with a 0.05 M potassium hydrogen phthalate solution. Gran's method[31] was used to confirm the absence of carbonate in the sodium hydroxide standard solution (carbonate content 0.13%). The perchloric acid solution was standardized by titration with NaOH. All solutions were adjusted to an ionic strength of 0.1 M with $NaClO_4$. The temperature was maintained by circulating thermostated water through the outer jacket of the cell. All measurements were carried out while a constant atmosphere of nitrogen was maintained above the solution. The concentration of complexes was 1.0×10^{-3} M, and the ionic strength was kept constant at 0.1 M by $NaClO_4$. Species distribution calculations and determination of the corresponding protonation equilibrium and stability constants were performed using the computer program TITFIT.[32]

NMR Measurements. The water exchange measurements were performed with 21 or 25 mM complex solutions. The complex was dissolved in 0.72 mL of a prepared buffer solution (TAPS or BIS−TRIS, 0.28 M in degassed Millipore water) of selected pH under a nitrogen atmosphere; 0.08 mL of 10 at.% $H_2{}^{17}O$-enriched water purchased from Deutero GmbH was added, and the pH of the solutions was checked on a Mettler Delta 350 pH meter with a combined glass electrode that was calibrated with standard buffer solutions (pH 4, 7, and 10). The solution was once more degassed by bubbling nitrogen through it for about 1 min and transferred to the NMR tube under nitrogen using Schlenk techniques.

Variable-temperature/pressure Fourier transform ^{17}O NMR spectra were recorded at a frequency of 54.24 MHz on a Bruker Avance DRX 400WB spectrometer equipped with a superconducting BC-94/89 magnet system. The temperature dependence of the ^{17}O line broadening for each system was measured over a temperature range from 278.2 to 358.2 K. A homemade high-pressure probe described in the literature was used for the variable-pressure experiments.[33] A standard 5 mm NMR tube cut to a length of 45 mm was used for the sample solutions in the high pressure measurements.

(31) (a) Gran, G. *Analyst* **1952**, *77*, 661−671. (b) Gran, G. *Anal. Chim. Acta* **1988**, *206*, 111−123. (c) Martell, A. E.; Motekaitis, R. J. *Determination and Use of Stability Constants*; VCH: Weinheim, Germany, 1992.

(32) Zuberbühler, A. D.; Kaden, T. A. *Talanta* **1982**, *29*, 201−206.

(33) Zahl, A.; Neubrand, A.; Aygen, S.; van Eldik, R. *Rev. Sci. Instrum.* **1994**, *65*, 882−886.

Data Treatment. From the observed line widths, where $\Delta\nu_{obs}$ and $\Delta\nu_{solv}$ are the half widths of the ^{17}O NMR signal of the solvent in the presence and absence of the Mn(II) complex, the reduced transverse relaxation rates $1/T_{2r}$ can be calculated for each temperature and pressure; $\Delta\nu_{solv}$ was found to be negligible and was set to zero because of the large line broadenings caused by the Mn(II) ion. According to the Swift and Connick equation (eq 2),[34] T_{2r} is related to τ_m, the mean coordinated solvent lifetime, and T_{2m}, the transverse relaxation time of coordinated water in the inner sphere of Mn(II) in the absence of chemical exchange. The exchange rate constant between coordinated and bulk water, k_{ex}, is $1/\tau_m$.

$$\frac{1}{T_{2r}} = \frac{\pi}{P_m}(\Delta\nu_{obsd} - \Delta\nu_{solv}) = \frac{1}{\tau_m}\left(\frac{T_{2m}^{-2} + (T_{2m}\tau_m)^{-1} + \Delta\omega_m^2}{(T_{2m}^{-1} + \tau_m^{-1})^2 + \Delta\omega_m^2}\right) + \frac{1}{T_{2os}} \quad (2)$$

P_m is the mole fraction of solvent in the exchanging site compared to the bulk solvent (eq 3, with n = number of coordinated water molecules); $\Delta\omega_m$ is the difference between the resonance frequency of oxygen-17 nuclei of solvent in the metal ion first coordination sphere and in the bulk. The outer-sphere contributions to T_{2r}, arising from long-range interactions of the paramagnetic unpaired electron of the manganese complex with the water outside the first coordination sphere, are represented by T_{2os}.

$$P_m = \frac{n\cdot[\text{complex}]}{[H_2O]} \quad (3)$$

The temperature dependence of $\Delta\omega_m$ was assumed to be the simple reciprocal function A/T,[35] where A was determined as a parameter in the treatment of the line broadening data.

The contribution of $1/T_{2m}$ and $1/T_{2os}$ was found to be negligible in the studied systems, so that eq 2 is reduced to eq 4. The solvent exchange rate constant, k_{ex}, is given by the Eyring equation (eq 5).

$$\frac{1}{T_{2r}} = \frac{1}{\tau_m}\left(\frac{\Delta\omega_m^2}{\tau_m^{-2} + \Delta\omega_m^2}\right) \quad (4)$$

$$k_{ex} = \frac{1}{\tau_m} = \frac{k_B T}{h}\exp\left(\frac{T\Delta S^{\ddagger} - \Delta H^{\ddagger}}{RT}\right) \quad (5)$$

The exchange rate constant is assumed to have a simple pressure dependence given by eq 6, where k_0 is the rate constant for solvent exchange at zero pressure. The reduced relaxation time T_{2r} and the value of $\Delta\omega_m$ (calculated using the value of A determined from the temperature dependence and assumed to be pressure independent) were substituted into eq 4 to determine k_{ex} at each pressure. In all cases, plots of $\ln(k_{ex}/s^{-1})$ versus p were linear within the experimental error, and the volumes of activation could be calculated directly from the slope.

$$k_{ex} = k_0\exp\left(-\frac{\Delta V^{\ddagger}}{RT}p\right) \quad (6)$$

Quantum Chemical Methods. All structures have been preoptimized at the UHF/LANL2MB[36−38] level of theory and characterized as minima, transition structures, or higher-order saddle points by computation of vibrational frequencies. We performed hybrid density functional structure optimizations using the B3LYP functional[39] and the LANL2DZ basis set with effective core potentials,[38,40] augmented with polarization functions on nonhydrogen atoms.[41] The performance at this level (denoted as B3LYP/LANL2DZp) has been documented by us and others.[42] Corrections for zero-point vibrational energy (UHF/LANL2MB) were made, and all wave functions were tested for stability. The GAUSSIAN suite of programs was used.[43]

Results and Discussion

Synthesis and Characterization of Complexes. The [Mn([15]aneN$_5$)Cl$_2$], [Mn(L1)Cl$_2$], and [Mn(L3)Cl$_2$] complexes, and the corresponding ligands were synthesized according to the published procedures.[10,15,28,29]

The new [Mn(L2)Cl$_2$] complex, which is an acyclic analog of [Mn(L1)Cl$_2$], was prepared by template synthesis[44] starting from MnCl$_2$, 2,6-diacetylpyridine, and *N*-methylethylenediamine. Its molecular structure is illustrated in Figure 1, and selected bond lengths and angles are listed in Table 2. Similar to the other Mn(II) complexes with macrocyclic N$_5$ ligands,[10,13−15] the [Mn(L2)Cl$_2$] complex (although with the acyclic pentadentate ligand) has a seven-coordinate pentagonal bipyramidal geometry with the chloro ligands in the axial

(34) (a) Swift, T. J.; Connick, R. E. *J. Chem. Phys.* **1962**, *37*, 307−320. (b) Swift, T. J.; Connick, R. E. *J. Chem. Phys.* **1964**, *41*, 2553−2554.

(35) (a) Bloembergen, N. *J. Chem. Phys.* **1957**, *27*, 572−573. (b) Bloembergen, N. *J. Chem. Phys.* **1957**, *27*, 595−596.

(36) Hehre, W. J.; Stewart, R. F.; Pople, J. A. *J. Chem. Phys.* **1969**, *51*, 2657−2664.

(37) Collins, J. B.; von Ragué Schleyer, P.; Binkley, J. S.; Pople, J. A. *J. Chem. Phys.* **1976**, *64*, 5142−5151.

(38) (a) Hay, P. J.; Wadt, W. R. *J. Chem. Phys.* **1985**, *82*, 270−283. (b) Hay, P. J.; Wadt, W. R. *J. Chem. Phys.* **1985**, *82*, 284−298. (c) Hay, P. J.; Wadt, W. R. *J. Chem. Phys.* **1985**, *82*, 299−310.

(39) (a) Becke, A. D. *J. Phys. Chem.* **1993**, *97*, 5648−5652. (b) Lee, C.; Yang, W.; Parr, R. G. *Phys. Rev. B.* **1988**, *37*, 785−789. (c) Stephens, P. J.; Devlin, F. J.; Chabalowski, C. F.; Frisch, M. J. *J. Phys. Chem.* **1994**, *98*, 11623−11627.

(40) Dunning, T. H., Jr.; Hay, P. J. *Mod. Theor. Chem.* **1976**, *3*, 1−28.

(41) Huzinaga, S., Ed. *Gaussian Basis Sets for Molecular Calculations*; Elsevier: Amsterdam, The Netherlands, 1984.

(42) For example, see: (a) Klaus, S.; Neumann, H.; Jiao, H.; Jacobi von Wangelin, A.; Gördes, D.; Strübing, D.; Hübner, S.; Hately, M.; Weckbecker, C.; Huthmacher, K.; Riermeier, T.; Beller, M. *J. Organomet. Chem.* **2004**, *689*, 3685−3700. (b) Saalfrank, R. W.; Deutscher, C.; Maid, H.; Ako, A. M.; Sperner, S.; Nakajima, T.; Bauer, W.; Hampel, F.; He*β*, B. A. N.; van Eikema Hommes, J. R.; Puchta, R.; Heinemann, F. W. *Chem.—Eur. J.* **2004**, *10*, 1899−1905. (c) Illner, P.; Zahl, A.; Puchta, R.; van Eikema Hommes, N. J. R.; Wasserscheid, P.; van Eldik, R. *J. Organomet. Chem.* **2005**, *690*, 3567−3576. (d) Scheurer, A.; Maid, H.; Hampel, F.; Saalfrank, R. W.; Toupet, L.; Mosset, P.; Puchta, R.; van Eikema Hommes, N. J. R. *Eur. J. Org. Chem.* **2005**, 2566−2574. (e) Galle, M.; Puchta, R.; van Eikema Hommes, N. J. R.; van Eldik, R. *Z. Phys. Chem.* **2006**, *220*, 511−523 and literature cited therein.

(43) Frisch, M. J.; Trucks, G. W.; Schlegel, H. B.; Scuseria, G. E.; Robb, M. A.; Cheeseman, J. R.; Montgomery, J. A., Jr.; Vreven, T.; Kudin, K. N.; Burant, J. C.; Millam, J. M.; Iyengar, S. S.; Tomasi, J.; Barone, V.; Mennucci, B.; Cossi, M.; Scalmani, G.; Rega, N.; Petersson, G. A.; Nakatsuji, H.; Hada, M.; Ehara, M.; Toyota, K.; Fukuda, R.; Hasegawa, J.; Ishida, M.; Nakajima, T.; Honda, Y.; Kitao, O.; Nakai, H.; Klene, M.; Li, X.; Knox, J. E.; Hratchian, H. P.; Cross, J. B.; Bakken, V.; Adamo, C.; Jaramillo, J.; Gomperts, R.; Stratmann, R. E.; Yazyev, O.; Austin, A. J.; Cammi, R.; Pomelli, C.; Ochterski, J. W.; Ayala, P. Y.; Morokuma, K.; Voth, G. A.; Salvador, P.; Dannenberg, J. J.; Zakrzewski, V. G.; Dapprich, S.; Daniels, A. D.; Strain, M. C.; Farkas, O.; Malick, D. K.; Rabuck, A. D., Raghavachari, K.; Foresman, J. B.; Ortiz, J. V.; Cui, Q.; Baboul, A. G.; Clifford, S.; Cioslowski, J.; Stefanov, B. B.; Liu, G.; Liashenko, A.; Piskorz, P.; Komaromi, I.; Martin, R. L.; Fox, D. J.; Keith, T.; Al-Laham, M. A.; Peng, C. Y.; Nanayakkara, A.; Challacombe, M.; Gill, P. M. W.; Johnson, B.; Chen, W.; Wong, M. W.; Gonzalez, C.; Pople, J. A. *Gaussian 03*, revision C.02, Gaussian, Inc.: Wallingford, CT, 2004.

(44) Brooker, S.; McKee, V. *J. Chem. Soc., Dalton Trans.* **1990**, 2397−2401.

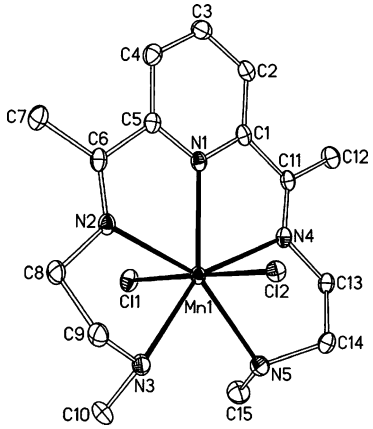

Figure 1. ORTEP drawing for $[Mn(L2)Cl_2]$, showing the labeling scheme and the 50% probability ellipsoids for the non-hydrogen atoms.

Table 2. Selected Bond Distances (Å) and Angles (deg) for $[Mn(L2)Cl_2]\cdot 0.22H_2O\cdot 1.78CH_3OH$[a]

bond distances			
Mn(1)−Cl(1)	2.5072(6)	Mn(1)−Cl(2)	2.6277(6)
Mn(1)−N(1)	2.347(2)	Mn(1)−N(2)	2.349(2)
Mn(1)−N(3)	2.394(2)	Mn(1)−N(4)	2.345(2)
Mn(1)−N(5)	2.428(2)		
bond angles			
Cl(1)−Mn(1)−Cl(2)	176.83(2)	Cl(1)−Mn(1)−N(1)	89.82(4)
Cl(1)−Mn(1)−N(2)	87.26(4)	Cl(1)−Mn(1)−N(3)	96.13(4)
Cl(1)−Mn(1)−N(4)	94.44(4)	Cl(1)−Mn(1)−N(5)	91.64(4)
Cl(2)−Mn(1)−N(1)	91.19(4)	Cl(2)−Mn(1)−N(2)	90.36(4)
Cl(2)−Mn(1)−N(3)	81.16(4)	Cl(2)−Mn(1)−N(4)	88.72(4)
Cl(2)−Mn(1)−N(5)	89.57(4)	N(1)−Mn(1)−N(2)	67.08(6)
N(1)−Mn(1)−N(3)	139.12(6)	N(1)−Mn(1)−N(4)	67.66(6)
N(1)−Mn(1)−N(5)	139.09(6)	N(2)−Mn(1)−N(3)	72.85(6)
N(2)−Mn(1)−N(4)	134.70(6)	N(2)−Mn(1)−N(5)	153.83(6)
N(3)−Mn(1)−N(4)	150.99(6)	N(3)−Mn(1)−N(5)	81.29(6)
N(4)−Mn(1)−N(5)	71.46(6)		

hydrogen bonds

	d(D−H)	*d*(H···**A**)	*d*(D···**A**)	∠(**D**−H···**A**)
N3−H3···Cl2[a]	0.93	2.56	3.420(2)	154
N5−H5···Cl2[a]	0.93	2.59	3.514(2)	175
O100−H100···Cl1	0.92	2.21	3.130(2)	172
O200−H200···Cl2	0.94	2.24	3.171(2)	170

[a] Symmetry code: $-x, -y+1, -z+1$.

positions. To our knowledge, this is the only seven-coordinate structure of manganese(II) with acyclic N_5 pentadentate. Within the crystal packing, two neighboring complex molecules are linked by hydrogen bonds (see Table 2) between the hydrogen atoms at N3 and N5 and the chloro ligand Cl2 of its neighbor to form dimers with the consequence that the methyl groups at these nitrogen atoms point in the same direction. This is in contrast to the complexes with macrocyclic N_5 ligands where the hydrogen atoms at the nitrogens are all in the trans direction.[10,13] The hydroxyl groups of the incorporated methanol molecules form hydrogen bonds to both of the chloro ligands (see Table 2). The pentagonal MnN_5 plane is only slightly distorted, the largest deviations from a least-squares plane calculated through the central Mn and the five N donor atoms are observed for N3 being 0.148(1) Å below and N5 being 0.114(1) Å above the plane. In comparison with its macrocyclic analog $[Mn(L1)(H_2O)_2]$,[29] the structure of $[Mn(L2)Cl_2]$ differs significantly in the Mn−N distances with values ranging from 2.345(2) to 2.428(2) Å. These Mn−N distances are significantly longer than in $[Mn(L1)(H_2O)_2]$, where they are between 2.254(2) and 2.316(2) Å.[29] However, in the structure of the Mn(II) complex derived from a larger 17-membered macrocycle with two SCN^- ligands in the axial positions, the Mn−N(macrocycle) distances (ranging from 2.311(5) to 2.429(6) Å)[45] are similar to those in $[Mn(L2)Cl_2]$. The acyclic and more flexible nature of the N_5 pentadentate ligand, together with the negatively charged ligands in the axial positions, results in longer Mn−N(equatorial) bond distances.

Scheme 3. Synthesis of $[Mn(L1)Cl_2]$, $[Mn(L3)Cl_2]$ and $[Mn(L4)Cl_2]$

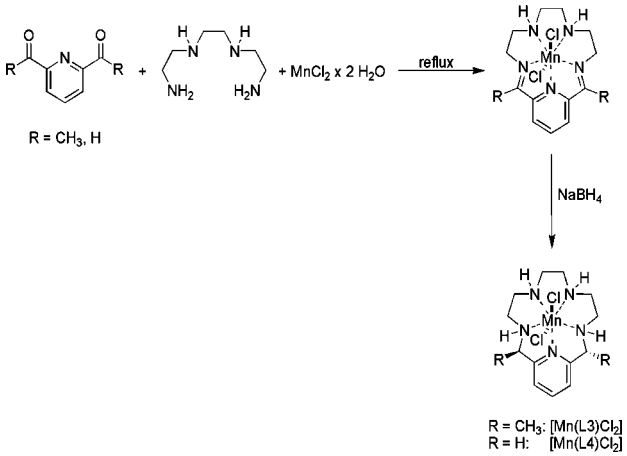

The $[Mn(L2)Cl_2]$ complex was synthesized with an idea to increase the flexibility of the L1 ligand while keeping the double bonds in its structure and then to compare the water-exchange processes for $[Mn(L1)Cl_2]$, $[Mn(L2)Cl_2]$, and $[Mn(L3)Cl_2]$. Unfortunately, although $[Mn(L2)Cl_2]$ is stable in a methanol solution for weeks, the acyclic nature of L2 gives the complex low stability in aqueous solution. The complex decomposes, presumably through hydrolysis of the C=N bonds, and water-exchange measurements could not be performed. However, we managed to perform a potentiometric titration of $[Mn(L2)Cl_2]$ (at room temperature under a nitrogen atmosphere, see below) to clarify its behavior in aqueous solution.

$[Mn(L3)Cl_2]$ was previously synthesized by catalytic reduction of $[Mn(L1)Cl_2]$ using a Ni−Al alloy in aqueous NaOH.[46] However, we found that the reduction with sodium borohydride in anhydrous EtOH is a more suitable synthetic method.[15]

$[Mn(L4)Cl_2]$ was obtained from 2,6-pyridinedicarboxaldehyde, triethylenetetramine, and manganese chloride via a template synthesis and a reduction with sodium borohydride according to the synthesis of $[Mn(L3)Cl_2]$ (Scheme 3). This synthetic route is much less extensive than the synthesis of the ligand via the Richman−Atkins procedure.[47] For [15]-aneN_5 (1,4,7,10,13-pentaazacyclopentadecane), however, the Richman−Atkins procedure was used in a relatively convenient modification published by Kovacs et al.,[28] and the

(45) Drew, M. G. B.; bin Othman, A. H.; McFall, S. G.; McIlroy, P. D. A.; Nelson, S. M. *J. Chem. Soc., Dalton Trans.* **1977**, 438−446.
(46) Jackels, S. C.; Durham, M. M.; Newton, J. E.; Henninger, T. C. *Inorg. Chem.* **1992**, *31*, 234−239.
(47) Stetter, H.; Frank, W.; Mertens, R. *Tetrahedron* **1981**, *37*, 767−772.

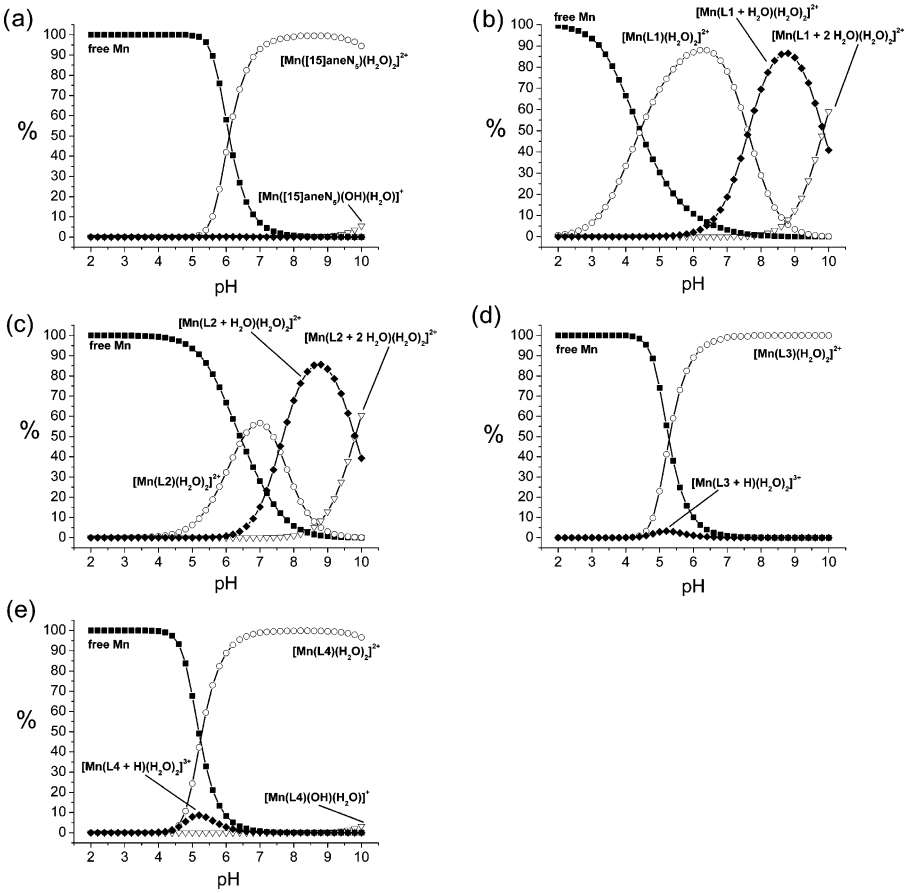

Figure 2. Species distribution in percent as a function of pH for the complexes (a) $[Mn([15]aneN_5)(H_2O)_2]$, (b) $[Mn(L1)(H_2O)_2]$, (c) $[Mn(L2)(H_2O)_2]$, (d) $[Mn(L3)(H_2O)_2]$, and (e) $[Mn(L4)(H_2O)_2]$ at 25 °C.

Table 3. Stability Constants for the Complexes and p*K* Values for their Ligands

complex	*T* (°C)	pK_1	pK_2	pK_3	pK(OH)$_1$	pK(OH)$_2$	log K_{ML}[a]	log K_{MHL}[a]	ref
$[Mn([15]aneN_5)(H_2O)_2]^{2+}$	25	5.99	9.51	10.38			10.55	3.66	*b*
$[Mn([15]aneN_5)(H_2O)_2]^{2+}$		5.93	9.29	10.31			10.85	5.04	13
$[Mn(L1)(H_2O)_2]^{2+}$	5				7.45	10.29	10.70	1.80	*b*
$[Mn(L1)(H_2O)_2]^{2+}$	25				7.62	9.84	10.50	-	*b*
$[Mn(L1)(H_2O)_2]^{2+}$	45				7.93		8.30	-	*b*
$[Mn(L2)(H_2O)_2]^{2+}$	25	-	-	-	7.57	9.81	10.47	-	*b*
$[Mn(L3)(H_2O)_2]^{2+}$	25	5.15	8.91	9.85			11.46	4.11	*b*
$[Mn(L4)(H_2O)_2]^{2+}$	25	5.27	8.82	9.11			11.12	4.51	*b*
$[Mn(L4)(H_2O)_2]^{2+}$		5.28	8.80	9.43			11.64	4.20	13

[a] $K_{ML} = [ML]/[M][L]$; $K_{MHL} = [MHL]/[ML][H]$. [b] This work

ligand was obtained in good yield. The $[Mn([15]aneN_5)Cl_2]$ complex was synthesized using the published procedure[10] and purified by column chromatography.

Potentiometric Titrations. Prior to the NMR studies it was important to examine the influence of the ligands on the stability and acid−base properties of the complexes to understand their solution behavior. This was achieved by potentiometric titrations. The calculated species distribution for all complexes obtained from the best fits to the titration data are shown in Figure 2. The pK_a values for the free ligands, as well as the stability constants for the complexes, are listed in Table 3. Similar to what was found in the literature,[13] $[15]aneN_5$, L3, and L4 exhibit three protonation equilibria, which correspond to the protonations of three secondary amine nitrogens. The pyridine ring-containing L3 and L4 ligands are less basic than $[15]aneN_5$, but the binding constants for $[Mn(L3)Cl_2]$ and $[Mn(L4)Cl_2]$ are somewhat higher than in the case of $[Mn([15]aneN_5)Cl_2]$ (Table 3). All three complexes are stable above a pH of around 5 and have a stable form with the monoprotonated ligand at one of the secondary amine nitrogen atoms.

The imine group-containing $[Mn(L1)Cl_2]$ and $[Mn(L2)Cl_2]$ complexes have quite different solution properties. They do not have a stable form with the monoprotonated ligand at 25 °C, since protonation immediately leads to hydrolysis of the ligand and decomposition of the complex. At 5 °C, a low stability form of the $[Mn(L1)Cl_2]$ complex (log K_{MHL} = 1.80) with a monoprotonated macrocycle could be observed. In the basic region however, we found two more pK values for both complexes, namely pK(OH)$_1$ = 7.6 and pK(OH)$_2$ = 9.8 (Figure 2b and 2c). In the UV−vis spectrum of $[Mn(L1)(H_2O)_2]$, we did not observe any spectral changes

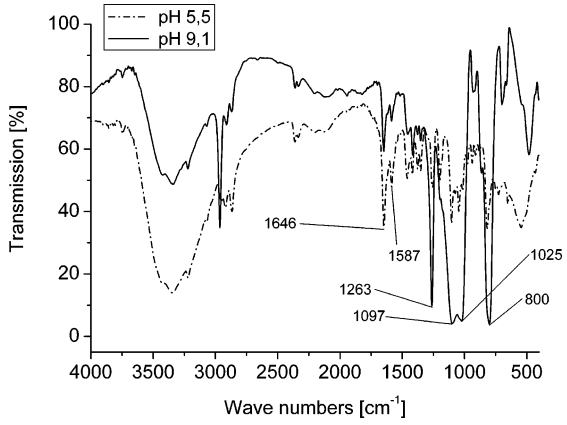

Figure 3. IR spectra of $[Mn(L1)(H_2O)_2]$ at pH 5.5 and 9.1.

by increasing the pH up to 11. Thus, direct changes in the manganese coordination sphere upon increased pH can be excluded. Therefore, the observed processes must be related to ligand changes, most probably to the base-catalyzed water addition to the imine bonds. A similar methanol and water addition to the imine bonds was already observed in the literature.[48−51] To verify this assumption, we obtained the crystals of $[Mn(L1)(H_2O)_2]$ from aqueous solutions at two different pH values (5.5 and 9.1), and their IR spectra were recorded (Figure 3). In the spectrum of the complex obtained at higher pH, strong bands at 1025 and 1097 cm^{-1}, which correspond to a stretch vibration of an alcoholic group (ν_{C-OH}) and a band at 1263 cm^{-1} (deformation of the OH bond, δ_{OH}) can be observed. In addition, the band for the deformation of the NH bond (800 cm^{-1}) gets stronger with higher pH, whereas the band for the stretch vibration of the imine bonds gets weaker (1646 cm^{-1}). Consequently, the following hydrolytic process for $[Mn(L1)(H_2O)_2]$ can be proposed

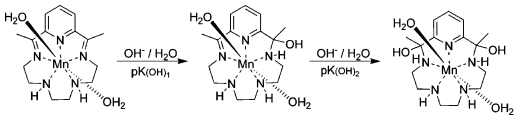

(7)

Similar processes were observed for $[Mn(L2)(H_2O)_2]$. The binding constants for $[Mn(L1)(H_2O)_2]$ and $[Mn(L2)(H_2O)_2]$ are just slightly lower than in the case of $[Mn([15]aneN_5)Cl_2]$. However, because of the acid- and base-catalyzed hydrolytic process, these two complexes are stable only in a quite narrow pH range. This complex solution behavior may also be a reason for the lack of catalytic SOD activity of the imine complexes.

For the water exchange measurements, it was necessary to examine the temperature dependence of the $pK(OH)_1$ and $pK(OH)_2$ values of $[Mn(L1)(H_2O)_2]$ (Table 3), since their shift would influence the species distribution during the NMR measurements (water exchange was measured in a temperature range between 5 and 85 °C). At lower temperature, the difference between $pK(OH)_1$ and $pK(OH)_2$ is somewhat bigger, whereas with increases in the temperature, these two values get closer. Thus, at 5 °C the $pK(OH)_1$ and $pK(OH)_2$ values are 7.45 and 10.29, respectively, whereas at 45 °C, these two processes occur in a concerted manner with overall $pK_{(OH)} = 7.93$. In any case, at pH = 6.1, the predominant species in solution at each temperature will be $[Mn(L1)(H_2O)_2]$ without changes at the imine bonds.

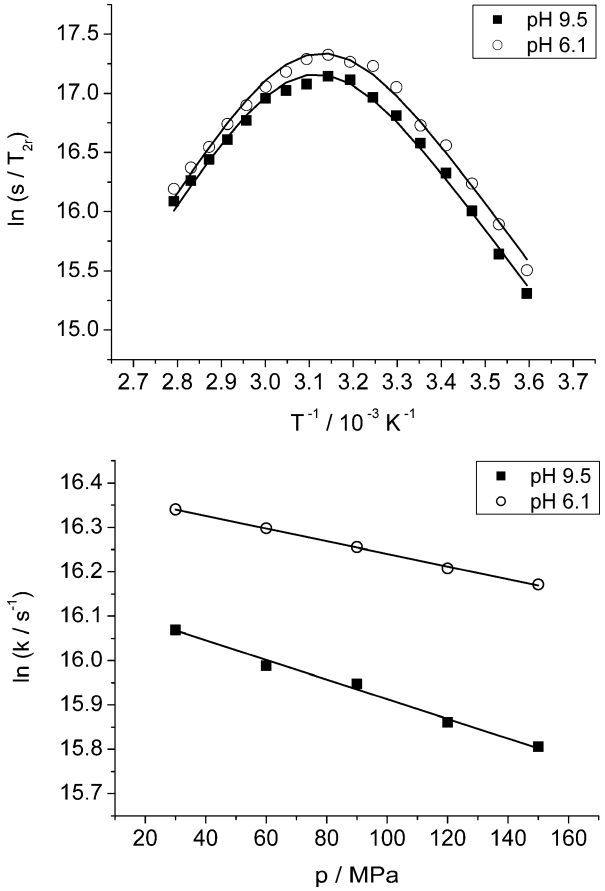

Figure 4. Temperature and pressure ($T = 288$ K) dependence for the water exchange on $[Mn(L1)(H_2O)_2]^{2+}$.

^{17}O NMR Water-Exchange Measurements. All studied complexes in aqueous solution are present as diaqua $[Mn(L)(H_2O)_2]^{2+}$ species, whereas two chloro ligands are replaced by water molecules in axial positions.[13,29] Rate constants for the water exchange reactions (eq 1) of the studied complexes and the corresponding activation parameters from the temperature- and pressure-dependent measurements are summarized in Table 4. The results of the temperature- and pressure-dependent measurements for $[Mn(L1)(H_2O)_2]^{2+}$ at two different pH values are shown in Figure 4 (for the other complexes, see the Supporting Information).

The values of the activation entropies and activation volumes are positive for all studied complexes, suggesting a dissociative nature (I_d) of the water-exchange mechanism. The activation enthalpies, $\Delta H^{\ddagger}$, are almost the same within the experimental error limits for all complexes and the applied *pH* of the solutions. The exchange rate constants, k_{ex}, however are influenced by the acceptor abilities of the spectator ligands. Water exchange on $[Mn(L1)(H_2O)_2]^{2+}$ is

(48) Nelson, S. M. *Pure Appl. Chem.* **1980**, *52*, 2461−2476.
(49) Cairns, C.; McFall, S. G.; Nelson, S. M.; Drew, M. G. B. *J. Chem. Soc., Dalton Trans.* **1979**, 446−453.
(50) Cook, D. H.; Fenton, D. E. *Inorg. Chim. Acta* **1977**, *25*, L95−L96.
(51) Pedrido, R.; Romero, M. J.; Bermejo, M. R.; Gonzalez-Noya, A. M.; Maneiro, M.; Rodriguez, M. J.; Zaragoza, G. *Dalton Trans.* **2006**, 5304−5314.

Table 4. Activation Parameters and Rate Constants for the Water Exchange Reaction of $[Mn(L1)(H_2O)_2]^{2+}$, $[Mn(L3)(H_2O)_2]^{2+}$, and $[Mn(L4)(H_2O)_2]^{2+}$ and Literature Values for $[Mn(H_2O)_6]^{2+}$

complex	pH	k_{ex}(298 K) ($\times 10^7$ s^{-1})	$\Delta H^{\ddagger}$(kJ mol^{-1})	$\Delta S^{\ddagger}$(J K^{-1} mol^{-1})	$\Delta V^{\ddagger}$(cm^3 mol^{-1})	ref
$[Mn(H_2O)_6]^{2+}$		2.1 ± 0.1	32.9 ± 1.3	$+5.7 \pm 5.0$	-5.4 ± 0.1	21
$[Mn(L1)(H_2O)_2]^{2+}$	6.1	2.0 ± 0.1	39.8 ± 1.3	$+28.6 \pm 4.4$	$+3.4 \pm 0.1$	this work
$[Mn(L1)(H_2O)_2]^{2+}$	7.6	1.7 ± 0.1	35.9 ± 1.7	$+13.6 \pm 5.8$		this work
$[Mn(L1)(H_2O)_2]^{2+}$	8.7	1.7 ± 0.1	40.3 ± 1.0	$+28.8 \pm 3.5$		this work
$[Mn(L1)(H_2O)_2]^{2+}$	9.5	1.6 ± 0.1	39.5 ± 1.1	$+25.7 \pm 3.8$	$+5.3 \pm 0.2$	this work
$[Mn(L3)(H_2O)_2]^{2+}$	7.7	5.3 ± 0.3	37.2 ± 0.4	$+27.6 \pm 1.5$	$+5.2 \pm 0.7$	this work
$[Mn(L3)(H_2O)_2]^{2+}$	10.9	5.8 ± 0.3	33.3 ± 0.6	$+15.2 \pm 1.9$	$+3.4 \pm 0.7$	this work
$[Mn(L4)(H_2O)_2]^{2+}$	8.0	4.7 ± 0.3	39.1 ± 0.6	$+33.0 \pm 2.1$	$+3.2 \pm 0.1$	this work
$[Mn([15]aneN_5)(H_2O)_2]^{2+}$	8.0	≥ 10				this work

about three times slower than in the case of $[Mn(L3)(H_2O)_2]^{2+}$ and $[Mn(L4)(H_2O)_2]^{2+}$, which have nearly the same exchange rate constants. Since the studied complexes exhibit a dissociative mode of the water-exchange process, the extended π-acceptor system of the $[Mn(L1)(H_2O)_2]^{2+}$ complex leads to a less labile $Mn-OH_2$ bond and to a slower reaction. The effect of the π-acceptor abilities of the L1 and L3 ligands on the $Mn-OH_2$ bond lability is also illustrated by the corresponding average $Mn-OH_2$ bond distance, which is somewhat shorter in the crystal structure of $[Mn(L1)(H_2O)_2]^{2+}$ (2.254 Å)[29] than in the structure of $[Mn(L3)(H_2O)_2]^{2+}$ (2.261 Å).[30] A trial to measure the water-exchange reaction of $[Mn([15]aneN_5)(H_2O)_2]^{2+}$ (Figure S10 in Supporting Information) resulted in an almost linear $\ln(1/T_{2r})$ versus $1/T$ curve. Such a curve cannot be properly analyzed; however, it clearly shows that the water-exchange process is faster in the case of $[Mn([15]aneN_5)(H_2O)_2]^{2+}$, with a rate constant of $\geq 1 \times 10^8$ s^{-1}. The lack of pyridine ring in the $[15]aneN_5$ ligand results in its decreased π-acceptor ability and consequently leads to the labilization of the coordinated water molecule. In contrast, the pH has no influence on the exchange reaction rates of the studied complexes. This suggests that in the applied pH ranges there are no changes in the manganese(II) coordination sphere. Even in the case of $[Mn(L1)(H_2O)_2]^{2+}$, where at pH values higher than 7.6, the predominant species possesses the hydrolyzed form of the L1 ligand (eq 6), the exchange rate constants are consistent within the experimental error. This can be related to the fact that the new electron-withdrawing hydroxyl group compensates for the decrease in π-acceptor ability of the pentadentate ligand upon addition of OH^- to the double bond. A trial to perform the measurements of $[Mn(L1)(H_2O)_2]^{2+}$ above pH 10 failed because of the decomposition of the complex at higher pH levels.

In the literature, there are only few studies on the water-exchange processes of the manganese(II) species in general,[21,24,25,52,53] and the only seven-coordinate Mn(II) complexes studied are $[Mn(EDTA)(H_2O)]^{2-}$ and its derivatives.[24-27] However, the volume of activation for the water-exchange reaction was reported only for six-coordinate $[Mn(H_2O)_6]^{2+}$ [21] and $[Mn^{II}_2(ENOTA)(H_2O)_2]$ (ENOTA = triazacyclononane-based ligand).[53] In water-exchange reactions of transition metal ions, the reactivity is strongly dependent on the electronic occupancy of their d orbitals.[54] As a consequence donor or acceptor abilities of the spectator ligands can affect the lability and the mechanism of the solvent exchange process. For seven-coordinate complexes, one would expect a dissociative mechanism for the exchange of the coordinated water molecule, which we have now shown to be so in this paper. This difference between six- and seven-coordinate Mn(II) species is clearly represented by the negative and positive values of the activation volumes for six-coordinate $[Mn(H_2O)_6]^{2+}$ ($\Delta V^{\ddagger} = -5.4$ cm^3 mol^{-1})[21] and $[Mn^{II}_2(ENOTA)(H_2O)_2]$ ($\Delta V^{\ddagger} = -10.7$ cm^3 mol^{-1})[53] and the studied seven-coordinate complexes (Table 4), respectively, since the activation volume is a more sensitive parameter than $\Delta H^{\ddagger}$ and $\Delta S^{\ddagger}$, leading to a better understanding of the nature of the substitution processes. The exchange rate constant of $[Mn(EDTA)(H_2O)]^{2-}$ is reported to be $(4.4 \pm 0.3) \times 10^8$ s^{-1} (298 K),[24] which is much faster than in the case of the complexes studied in this paper. This is caused by the strong σ-donor ability and high negative charge of the EDTA ligand and also by the fact that in $[Mn(EDTA)(H_2O)]^{2-}$ the water molecule is in the sterically crowded equatorial plane with five donor atoms, whereas in our complexes water molecules are in the axial positions. In the case of six-coordinate species, where an associative mechanism for the water exchange would be expected, the increase in the π-acceptor ability of the spectator ligands has an opposite effect than in the case of seven-coordinate complexes, namely, it accelerates the exchange rate. It can be clearly observed if we compare the water-exchange rate constants for $[Mn(H_2O)_6]^{2+}$, $[Mn(phen)(H_2O)_4]^{2+}$, and $[Mn(phen)_2(H_2O)_2]^{2+}$, which are found to be $(5.8 \pm 0.1) \times 10^6$ (calculated for 0 °C from literature data),[21] $(13 \pm 2) \times 10^6$, and $(31 \pm 3) \times 10^6$ s^{-1} (both at 0 °C), respectively.[52]

DFT Calculations. DFT calculations were performed for the $[Mn(L1)(H_2O)_2]^{2+}$, $[Mn(L2)(H_2O)_2]^{2+}$, $[Mn(L3)(H_2O)_2]^{2+}$, and $[Mn(L4)(H_2O)_2]^{2+}$ complexes, as well as for their corresponding six-coordinate structures $[Mn(L)(H_2O)]^{2+}$, to compare the energy required for the water dissociation (ΔE) and the complex reactivity according to a dissociative mechanism with the six-coordinate species as intermediate structures. All seven-coordinate complexes show C_2 symmetry, and the axial positions are equivalent. The ΔE values are given in Table 5, and the calculated structures are shown in Figure 5. From Table 5, it can be seen that for the three

(52) Grant, M.; Dodgen, H. W.; Hunt, J. P. *Inorg. Chem.* **1971**, *10*, 71−73.
(53) Balogh, E.; He, Z.; Hsieh, W.; Liu, S.; Toth, E. *Inorg. Chem.* **2007**, *46*, 238−250.
(54) Dunand, F. A.; Helm, L.; Merbach, A. E. *Adv. Inorg. Chem.* **2003**, *54*, 1−69.

Table 5. Calculated Energies for the Dissociation of One Water Molecule for the Complexes $[Mn(L1)(H_2O)_2]^{2+}$, $[Mn(L2)(H_2O)_2]^{2+}$, $[Mn(L3)(H_2O)_2]^{2+}$, and $[Mn(L4)(H_2O)_2]^{2+}$

complex	ΔE (kcal mol^{-1})
$[Mn(L1)(H_2O)_2]^{2+}$	17.5
$[Mn(L2)(H_2O)_2]^{2+}$	30.4
$[Mn(L3)(H_2O)_2]^{2+}$	16.2
$[Mn(L4)(H_2O)_2]^{2+}$	18.4

complexes with cyclic ligands the energy differences are almost the same, whereas in the case of acyclic ligand ΔE is significantly different. Ligand L3 shows the most distinct folding, with the corresponding six-coordinate structure showing a pseudo-octahedral geometry. However, the L1 and L4 ligands do not show any prominent folding. For the L1 ligand it is to be expected, since the imine bonds make the ligand quite rigid and unflexible. Surprisingly, also the L4 ligand shows a rigid behavior, and the ligand is not able to fold and form a pseudo-octahedral coordination sphere. The somewhat lower ΔE value for $[Mn(L3)(H_2O)_2]^{2+}$ can be interpreted in terms of the better conformational adaptation of L3 to the six-coordinate geometry.

In the calculated seven-coordinate structure of $[Mn(L2)(H_2O)_2]^{2+}$ (Figure 5b), the methyl groups at the terminal nitrogen atoms point in the opposite directions, which is different from what has been observed in the crystal structure of $[Mn(L2)Cl_2]$. This is a nice example how the crystal packing effects, namely, interactions between two neighbored complex molecules via hydrogen bonds can influence the ligand conformation in the solid state. The acyclic L2 ligand, despite possessing two imine groups, is much more flexible than the studied macrocyclic ligands and interestingly, as a result of DFT calculations, the dissociation of one water molecule resulted in a five-coordinate square-pyramidal geometry around the Mn(II) center (Figure 5b). Flexibility of the ligand pendent arms enabled coordination of one of the terminal secondary amine groups in the axial position, whereas the rigidity of the imine group from the same arm disabled its coordination, allowing binding of the water molecule in the equatorial plane. The hydrogen bond between the imine group and the water molecule stabilizes its coordination. This change from the seven- to five-coordination geometry upon water dissociation, namely, a break of the additional bond (Mn−N(imine)) is a reason for the higher ΔE in the case of $[Mn(L2)(H_2O)_2]^{2+}$ (Table 5). Most likely, more than half of the ΔE value comes from the energy required for the Mn−imine bond breaking (∼15−20 kcal/mol).[55] Interestingly, in a hypothetical saturated analog of the $[Mn(L2)(H_2O)_2]^{2+}$ complex,[56] resulting from the reduction of imine bonds, a lack of the imine groups and the corresponding increase of ligand flexibility enable formation of the six-coordinate octahedral structure upon dissociation of one water molecule (Figure S11, Supporting Information). The calculated ΔE value in this case is significantly smaller, 10.57 kcal/mol, which is to be expected since there is no additional bond breaking and the prominent ligand flexibility assists in its favorable conformational adaptation to the six-coordinate geometry.

Despite the fact that the $[Mn(L2)Cl_2]$ complex is quite unstable in water, the increased flexibility of the acyclic ligand and possibility for the formation of the square-pyramidal structure with the vacant axial coordination site is quite promising for the further development of this class of ligands and corresponding SOD active complexes.

The energies for the complete dissociation of one water molecule (Table 5) cannot be correlated with the water exchange rate constants of the $[Mn(L1)(H_2O)_2]^{2+}$, $[Mn(L3)(H_2O)_2]^{2+}$, and $[Mn(L4)(H_2O)_2]^{2+}$ complexes. This means that the water dissociation is not a limiting step in the solvent exchange mechanism of the studied complexes. The π-acceptor ability of the ligands, which enables the partial entrance of another H_2O molecule, is responsible for the changes in the rate constants and also for the fact that the exchange mechanism is not a pure dissociative but more interchange one. ΔE is also not possible to correlate with the catalytic rate constants published in the literature. In contrast, the complex with the strongest folded ligand, $[Mn(L3)(H_2O)_2]^{2+}$, has a lower k_{cat} value (1×10^7 M^{-1} s^{-1}) than $[Mn(L4)(H_2O)_2]^{2+}$ (3.65×10^7 M^{-1} s^{-1}),[9] where the ligand is nearly unable to fold and form a pseudo-octahedral coordination sphere.

The attempt to calculate the seven-coordinate structure of $[Mn([15]aneN_5)(H_2O)_2]$ resulted in a six-coordinate geometry around Mn(II), where only one water molecule is coordinated to the manganese center and the second noncoordinated water molecule, which is in a sort of second coordination sphere, forms hydrogen bonds with the $[15]aneN_5$ ligand. This can be correlated with the higher substitution lability of the $[Mn([15]aneN_5)(H_2O)_2]$ complex in aqueous solution, which is reflected in the faster water exchange process as experimentally observed (Table 4).

Comparison with SOD activity. It has been reported that in the inner-sphere SOD catalytic pathway (Scheme 1) the rate-determining step is formation of the six-coordinate intermediate upon release of water.[10,14,15] Since in that case the water-exchange process should be the rate limiting one, the inner-sphere catalytic rate constants were correlated with the water-exchange rate constants on $[Mn(H_2O)_6]^{2+}$.[10,14] However, it seems that it is not possible to draw a direct correlation between these rate constants. First, the inner-sphere rate constant k_{IS} (which is pH independent) according to the observed rate law for dismutation of superoxide[57] has the unit M^{-1} s^{-1}, whereas the unit of the water-exchange rate constant is s^{-1}. Therefore the values for k_{IS}, which are in general for all reported complexes in the $0.15-3.98 \times 10^7$ M^{-1} s^{-1} range and in particular for the $[Mn([15]aneN_5)Cl_2]$ and $[Mn(L4)Cl_2]$ complexes 0.91×10^7 and 1.01×10^7 M^{-1} s^{-1}, respectively,[13,20] are not directly comparable with $k_{ex} = 2.1 \times 10^7$ s^{-1} for $[Mn(H_2O)_6]^{2+}$. (The k_{IS} value

(55) (a) Mortimer, C. T.; McNaughton, J. L. *Thermochim. Acta* **1974**, *10*, 207−210. (b) Kappes, M. M.; Staley, R. H. *J. Am. Chem. Soc.* **1982**, *104*, 1813−1819.

(56) Trials to synthesize this complex via reduction of the imine bonds were not successful so far.

(57) From refs 2 and 3, $V = -d[O_2^{\bullet-}]/dt = [Mn][O_2^{\bullet-}]\{k_H^+[H^+] + k_{ind}\}$, $k_{ind} = 2k_{IS}$, and $k_H^+ = 2k_{OS}/K_a$.

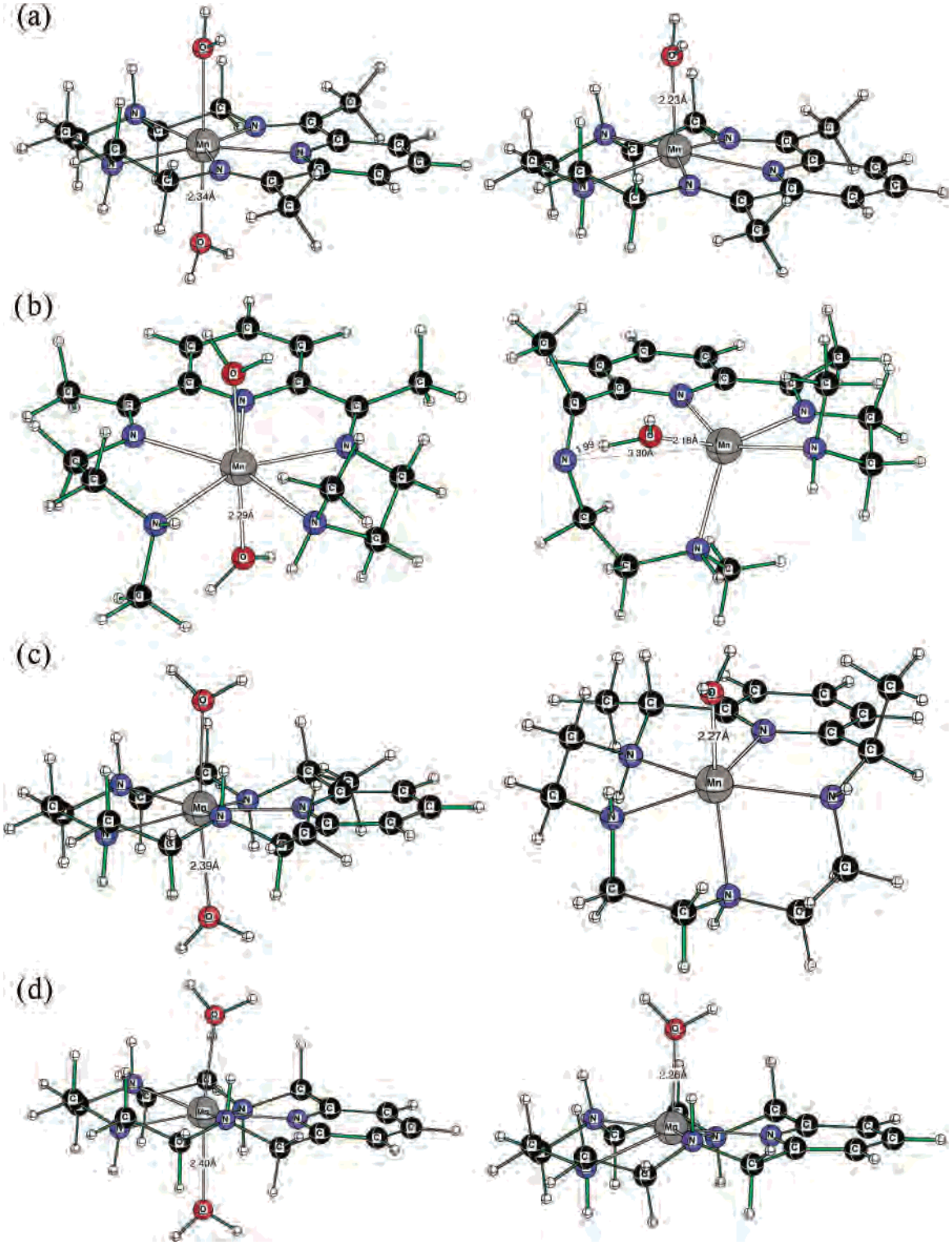

Figure 5. Structures calculated with DFT methods (B3LYP/LANL2DZp) for the seven-coordinate diaqua complexes (a) $[Mn(L1)(H_2O)_2]^{2+}$ (b) $[Mn(L2)(H_2O)_2]^{2+}$ (c) $[Mn(L3)(H_2O)_2]^{2+}$, and (d) $[Mn(L4)(H_2O)_2]^{2+}$ (on the left) and the corresponding six-coordinate species after the loss of one water molecule on the right.

for $[Mn(L3)Cl_2]$ was not reported in the literature, and $[Mn(L1)Cl_2]$ is known to be SOD inactive.) One should divide k_{ex} by $[H_2O]$ (55.5 M) to obtain comparable values. In that way, the values for k_{IS} would be usually much higher than the corresponding value of k_{ex}, suggesting a somewhat different mechanism for the inner-sphere SOD catalytic pathway of seven-coordinate Mn(II) complexes. It would be more appropriate to compare k_{IS} with k_{ex} of the particular seven-coordinate complex and not with the value of k_{ex} for the six-coordinate $[Mn(H_2O)_6]^{2+}$, since we have shown that k_{ex} can vary by almost a factor of 10 (Table 4). In the case of the $[Mn(L4)Cl_2]$ complex, $k_{ex}/[H_2O] = 0.85 \times 10^6\ M^{-1}\ s^{-1}$, whereas in the case of $[Mn([15]aneN_5)Cl_2]$ $k_{ex}/[H_2O] \geq 1.8 \times 10^6\ M^{-1}\ s^{-1}$. These values are almost 1 order of

magnitude lower than corresponding k_{IS} values, suggesting that the water release cannot be a rate-determining step (otherwise the inner-sphere SOD catalytic pathway should have consequently been slower than the experimentally observed one). Additionally, these two complexes have almost the same values of k_{IS}; however k_{ex} differs significantly. Such discrepancies could be explained in terms of an interchange (I_d) mechanism for the substitution of the water molecule by the incoming superoxide anion (as we have found for the water exchange process) with the formation of the outer-sphere precursor complex, rather than in terms of a limiting dissociative mechanism with a six-coordinate intermediate. In that way, the obtained k_{IS} constant would depend not only on k_{ex} but also on an outer-sphere precursor formation constant K_{OS}, where $k_{IS} = K_{OS}k_{ex}$. The interchange character of the water exchange mechanism of the studied seven-coordinate complexes can also be a reason why there is no clear correlation between their rates for the exchange process and the energies required for the dissociation of the coordinated water molecule. It is not surprising that the substitution processes on seven-coordinate 3d metal ions follow an interchange, rather than a limiting dissociative mechanism. In the case of a seven-coordinate Fe(III) complex, we even found an associative interchange mechanism for the substitution of solvent molecules as a result of the high π-acceptor ability of the fully conjugated pentadentate ligand system present in its equatorial plane.[22,23]

Conclusions

Seven-coordinate Mn(II) complexes, with macrocyclic pentadentate derivatives of [15]aneN$_5$ in the equatorial plane and two water molecules in the axial positions, have been the subject of potentiometric, variable-temperature and -pressure ^{17}O NMR, and DFT studies. In addition the synthesis, potentiometric titration, and X-ray crystal structure of a new seven-coordinate Mn(II) complex with the acyclic pentadentate ligand has been reported. These complexes are interesting because they could be one of the best SOD mimetics[11,12,15,17] and potential human therapeutics for the treatment of diseases characterized by the overproduction of superoxide.[10,13−15] It was proposed that the water release and formation of a six-coordinate intermediate is the rate-limiting step in the overall inner-sphere catalytic superoxide dismutation pathway.[10,12] Therefore, it was of importance to assess the rate constants and corresponding activation parameters of the water-exchange process and to elucidate its mechanism. The positive values of activation entropies and especially of activation volumes (obtained for the first time for the seven-coordinate Mn(II) species) suggest an interchange dissociative (I_d) nature of the water exchange mechanism. The water exchange rate constants are mainly controlled by the π-acceptor abilities of the ligands and decrease with an increase of the ligand π-acceptor ability, which also confirms a dissociative character of the water exchange. Importantly, the second-order rate constants k_{IS} for the inner-sphere catalytic pathway[13,20] are significantly higher than the corresponding $k_{ex}/[H_2O]$ values for the water-exchange, suggesting that water release cannot be a rate-determining step. This can be explained in terms of an interchange (I_d) mechanism for the substitution of the water molecule on the seven-coordinate Mn(II) center, where the incoming superoxide anion also plays a role in the overall substitution process. Additionally, it has been postulated that the complexes with ligand systems containing imine groups do not have SOD activity[10,15] most probably because of the conformational rigidity and low ability to form a six-coordinate pseudo-octahedral intermediate upon release of one water molecule. However, our DFT calculations show that some of the SOD active complexes, without the imine groups in the macrocyclic ligand, also do not show significant conformational flexibility and do not have a pseudo-octahedral structure in the six-coordinated form but rather have the same pentagonal-pyramidal structure as does an SOD inactive complex. This suggests that conformational flexibility of the pentadentate ligand is not the key factor which assists in SOD activity. Furthermore, we have shown that the seven-coordinate complexes with acyclic imine-containing ligands have the potential to form the square-pyramidal intermediate structure, with a vacant axial coordination site, upon the release of one water molecule. This is a quite promising for the further development of complexes with acyclic pentadentate ligands as potential SOD mimetics.

Acknowledgment. The authors gratefully acknowledge financial support from the Deutsche Forschungsgemeinschaft within SFB 583 "Redox-active Metal Complexes". We thank Prof. Tim Clark for hosting this work in the CCC and the Regionales Rechenzentrum Erlangen (RRZE) for a generous allotment of computer time. We are also thankful to Prof. A. E. Merbach and Prof. R. van Eldik for helpful discussions.

Supporting Information Available: Water-exchange data and corresponding figures for all measured complexes, calculated structures for the saturated analog of $[Mn(L2)(H_2O)_2]^{2+}$, and full crystallographic details for complex $[Mn(L2)Cl_2]$ as crystallographic information file (CIF). This material is available free of charge via the Internet at http://pubs.acs.org.

IC061852O